

Application of Amino-Functionalized SBA-15 Type Mesoporous Silica in One-Pot Synthesis of Spirooxindoles

Ghodsii MOHAMMADI ZIARANI^{1,*}, Alireza BADIEI², Somayeh MOUSAVI¹, Negar LASHGARI², Afsaneh SHAHBAZI²

¹Department of Chemistry, Alzahra University, Vanak Square, P.O. Box 1993893973, Tehran, Iran

²School of Chemistry, College of Science, University of Tehran, Tehran, Iran

Abstract: Amino-functionalized SBA-15 (SBA-Pr-NH₂) has been used as a new basic nanocatalyst in the one-pot synthesis of spirooxindole derivatives via the three-component condensation reaction of isatins, activated methylene reagents, and dimedone in an aqueous medium. SBA-Pr-NH₂ has been established as an efficient heterogeneous nanoporous solid basic catalyst (pore size of 6 nm) that can be easily handled and removed from the reaction mixture by simple filtration, and also recovered and reused without noticeable loss of reactivity.

Key words: amino-functionalized SBA-15; spirooxindoles; isatin; nano-reactor; green synthesis

CLC number: O643 **Document code:** A

Received 15 August 2012. Accepted 11 September 2012.

*Corresponding author: Tel/Fax: +98-2188041344; E-mail: gmziarani@hotmail.com; gmohammadi@alzahra.ac.ir

This work was supported by Alzahra University and university of Tehran.

English edition available online at Elsevier ScienceDirect (<http://www.sciencedirect.com/science/journal/18722067>).

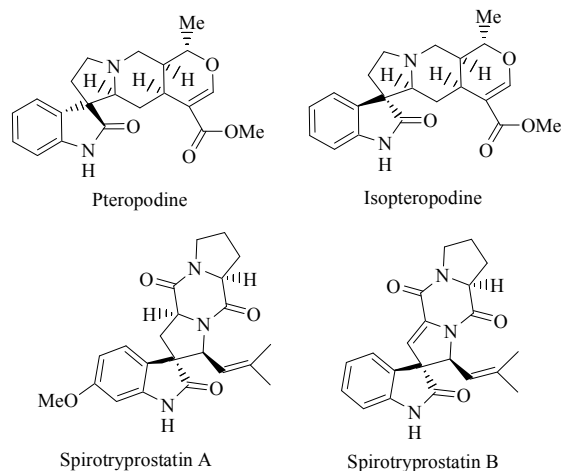
Spiro compounds composed of cyclic structures fused at a central carbon atom have recently been the subject of considerable attention because of their interesting conformational features and their structural implications on biological systems. Compounds of this structural class represent an important group of naturally occurring substances that are characterized by their extensive biological properties and applications [1]. The spirooxindole ring system is the core structure in a variety of pharmacologically active agents and natural alkaloids [2]. For example, pteropodine and isopteropodine have been shown to modulate the functions of muscarinic receptors in rats [3], whereas spirotryprostatin A and B have been identified as mammalian cell cycle inhibitors (Scheme 1) [4].

The spirooxindole derivatives have also demonstrated significant potential for use in a wide range of biological applications such as antimicrobial [5], antitumor [6], and therapeutic agents [7]. Of the heterocycles fused to a spirooxindole ring system, functionally substituted 4H-chromenes are of particular utility because they possess important biological activities.

Several methods have been developed for the synthesis of these heterocyclic skeletons. Isatin has been widely used in organic synthesis [8,9], with one example including the preparation of spirooxindole derivatives via a three-component condensation reaction of dimedone with activated methylene reagents in the presence of different catalysts such as InCl₃ [10], tetra-*n*-butylammonium fluo-

ride (TBAF) [11], β -cyclodextrin [12], NH₄Cl [13], triethylbenzylammonium chloride (TEBA) [14], and ethylenediamine diacetate (EDDA) [15].

Mesoporous solids have received considerable attention recently because of their unique features, such as their high specific surface area, large pore volume, controllable and narrowly distributed pore sizes, biocompatibility, and low levels of toxicity. These ordered mesoporous materials (OMMs) have been reported to have potential applications in several areas, including adsorption [16], chromatography [17], drug delivery [18], and catalysis [19]. Of the many



Scheme 1. Representative examples of spirooxindole-containing compounds.

different functionalized silica materials, amino-functionalized SBA-15 is one of the most important functionalized mesoporous materials because it has been used as catalyst in a variety of reactions [20,21]. Considering the biomedical applications of spirooxindole derivatives and in view of the limitations of the existing methods, we were encouraged to use SBA-Pr-NH₂ as a catalyst for the facile and efficient multicomponent synthesis of functionalized spirooxindoles.

1 Experimental

1.1 Materials and methods

All chemicals were obtained commercially and used without further purification. Pluronic P123 (PEO₂₀-PPO₇₀-PEO₂₀, $M_{ac} = 5800$) block copolymer non-ionic surfactant was purchased from Sigma Aldrich. Tetraethyl orthosilicate (TEOS, 98%), 3-aminopropyltrimethoxysilane (APTES, 99%), hydrochloric acid (HCl, 37%), and toluene were purchased from Merck (Germany). IR spectra were recorded from KBr disks using an FT-IR Bruker Tensor 27 instrument. Melting points were measured using the capillary tube method with an Electrothermal 9200 apparatus. ¹H NMR was run on a Bruker DPX at 500 MHz using TMS as an internal standard. Gas chromatography-mass spectrometry (GC-MS) analysis was performed on an Agilent 6890-5973 GC/MS detector. The low-angle powder X-ray diffraction (XRD) patterns were recorded over a range of $0.5^\circ < 2\theta < 8^\circ$ on a Philips X'pert MPD diffractometer equipped with a liquid nitrogen-cooled germanium solid-state detector using Cu K_α radiation (40 kV, 30 mA) at a step width of 0.02° . Nitrogen adsorption-desorption isotherms were measured at -196°C using a BELSORP-mini II. All samples were degassed at 100°C for 3 h under vacuum with an argon gas flow prior to analysis. The specific surface area (A_{BET}) was evaluated using the Brunauer-Emmett-Teller (BET) equation, and the pore size distribution (D_{BJH}) was obtained from the desorption branches by means of the Barrett-Joyner-Halenda (BJH) model, with the pore volume being taken at $p/p_0 = 0.995$. Fourier transform infrared spectra (FT-IR) were recorded within the $600\text{--}4000\text{ cm}^{-1}$ region on a Bruker Vector 22 infrared spectrophotometer to characterize the anchoring functional groups on the silica surface. Transmission electron microscopy (TEM) analysis was performed on a Tecnai G² F30 at 300 kV.

1.2 SBA-15 nanoporous silica synthesis and functionalization

The synthesis of SBA-15 was similar to that described previously in the literature [22,23] and involved the use of

Pluronic P123 nonionic surfactant as a structure directing agent and TEOS under acidic conditions. Surface modifications over the nanoporous silica with aminopropyl moieties were performed using the post-synthesis grafting method [24]. In a typical process, calcined SBA-15 (5 g) was activated at 200°C under vacuum for 5 h to remove any surface humidity and subsequently refluxed in dry toluene (150 ml). APTES (30.2 mmol) was then slowly added to the mixture and the reaction was refluxed at 110°C for a further 24 h. The mixture was then filtered and washed with toluene and any residual organosilane was removed by Soxhlet extraction in ethanol over a 24 h period. The resulting material was denoted as NH₂-SBA-15.

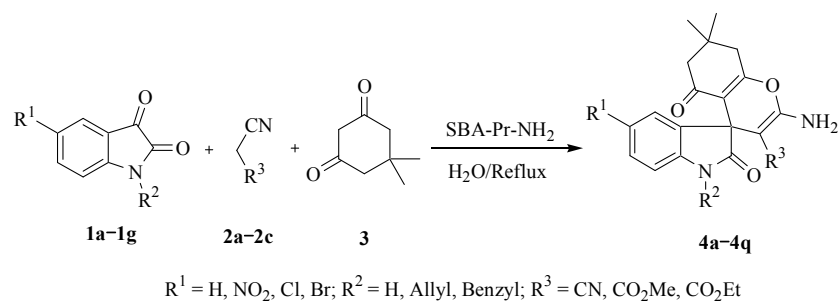
1.3 General procedure for the preparation of *N*-substituted isatins (1e–1g)

Isatin (10 mmol, 1.47 g) or 5-bromoisatin (10 mmol, 2.45 g), potassium carbonate (13 mmol, 1.82 g), and the corresponding alkyl halide (11 mmol) were dissolved in DMF (10 ml) and heated under reflux at 120°C . Upon completion of the reaction (monitored by TLC), the crude product was poured in iced water. If the product could be purified by recrystallization, the resulting solid was filtered and washed well with water before being purified by recrystallization from EtOH. If, however, an oily product was formed that resisted crystallization, it was dissolved in ethyl acetate and the organic layer was washed with water and then dried to give the pure product.

1.4 General procedure for the synthesis of spirooxindole derivatives (4a–4q)

The isatin derivative **1a–1g** (2 mmol), activated methylene reagent **2a–2c** (2 mmol), dimedone **3** (2 mmol), and SBA-Pr-NH₂ (0.02 g) were dissolved in water (5 ml) and refluxed (Scheme 2) for the appropriated length of time, as mentioned in Table 3. The progress of the reaction was monitored by TLC. Upon completion of the reaction, the mixture was cooled to room temperature and the crude product filtered off and washed with H₂O. The filter-cake was then collected and dissolved in hot ethanol, and the catalyst was removed by filtration. The filtrates were then cooled to afford pure crystals of the spirooxindole derivatives. The recovered catalyst could then be washed sequentially with diluted aqueous Et₃N solution, water, and acetone. Following a period of drying, the catalyst could be reused without any noticeable loss in reactivity.

Methyl-2-amino-5-oxo-7,7-dimethyl-spiro[(4H)-5,6,7,8-tetrahydrochromene-4,3'-(3'H)-5'-nitro-indol]-(1'H)-2'-one-3-carboxylate (**4f**). IR (KBr, cm^{-1}): 3379, 3189, 2954, 1727, 1685, 1620, 1522, 1445, 1329, 1213, 1090, 1059, 907, 746.



Scheme 2. Synthesis of spirooxindoles **4a–4q** in the presence of SBA-Pr-NH₂.

¹H NMR (500 MHz, DMSO-d₆): δ 10.95 (s, 1H, NH), 8.14 (br. s, 2H, NH₂), 7.74–7.93 (m, 1H, ArH), 6.91 (d, $J = 8.0$ Hz, 1H, ArH), 6.89 (d, $J = 8.1$ Hz, 1H, ArH), 3.32 (s, 3H, CH₃), 2.56 (d, $J = 15.8$ Hz, 2H, CH₂), 2.12 (d, $J = 15.9$ Hz, 1H, CH_AH_B), 2.09 (d, $J = 15.7$ Hz, 1H, CH_AH_B), 1.00 (s, 3H, CH₃), 0.98 (s, 3H, CH₃). EI-MS: 413 (M⁺), 354 (100), 329.

Methyl-2-amino-5-oxo-7,7-dimethyl-spiro[(4H)-5,6,7,8-tetrahydrochromene-4,3'-(3'H)-5'-chloro-indol]-(1'H)-2'-one-3-carboxylate (**4g**). IR (KBr, cm⁻¹): 3330, 3193, 3134, 2956, 2722, 1733, 1597, 1477, 1303, 1247, 1153, 1051, 963, 780. ¹H NMR (500 MHz, DMSO-d₆): δ 10.28 (s, 1H, NH), 7.82 (br. s, 2H, NH₂), 7.05–7.07 (m, 1H, ArH), 6.87 (d, $J = 8.0$ Hz, 1H, ArH), 6.70 (d, $J = 8.2$ Hz, 1H, ArH), 3.26 (s, 3H, CH₃), 2.52 (m, 2H, CH₂), 2.14 (d, $J = 15.8$ Hz, 1H, CH_AH_B), 2.07 (d, $J = 15.8$ Hz, 1H, CH_AH_B), 1.04 (s, 3H, CH₃), 0.97 (s, 3H, CH₃). EI-MS: 402 (M⁺), 343 (100), 318, 304, 260, 83, 55.

Methyl-2-amino-5-oxo-7,7-dimethyl-spiro[(4H)-5,6,7,8-tetrahydrochromene-4,3'-(3'H)-5'-bromo-indol]-(1'H)-2'-one-3-carboxylate (**4h**). IR (KBr, cm⁻¹): 3337, 3200, 2946, 1695, 1617, 1522, 1475, 1300, 1224, 1186, 1052, 906, 785. ¹H NMR (500 MHz, DMSO-d₆): δ 10.29 (s, 1H, NH), 7.85 (br. s, 2H, NH₂), 7.21 (d, $J = 7.6$ Hz, 1H, ArH), 6.66 (d, $J = 8.0$ Hz, 1H, ArH), 3.27 (s, 3H, CH₃), 2.53 (m, 2H, CH₂), 2.15 (d, $J = 15.8$ Hz, 1H, CH_AH_B), 2.08 (d, $J = 15.8$ Hz, 1H, CH_AH_B), 1.00 (s, 3H, CH₃), 0.96 (s, 3H, CH₃). EI-MS: 448 (M⁺), 389 (100), 362, 309, 281, 250, 83.

Ethyl-2-amino-5-oxo-7,7-dimethyl-spiro[(4H)-5,6,7,8-tetrahydrochromene-4,3'-(3'H)-5'-nitro-indol]-(1'H)-2'-one-3-carboxylate (**4j**). IR (KBr, cm⁻¹): 3522, 3367, 3255, 3190, 2958, 1725, 1686, 1621, 1524, 1470, 1332, 1216, 1170, 1058, 907, 748. ¹H NMR (500 MHz, CDCl₃): δ 10.04 (s, 1H, NH), 8.08 (s, 2H, NH₂), 6.91–7.71 (m, 3H, ArH), 3.87 (q, $J = 6.5$ Hz, 2H, CH₂), 2.49 (m, 2H, CH₂), 2.17 (d, $J = 16.1$ Hz, 1H, CH_AH_B), 2.08 (d, $J = 16.1$ Hz, 1H, CH_AH_B), 1.01 (s, 3H, CH₃), 0.89 (s, 3H, CH₃), 0.88 (t, $J = 7.1$ Hz, 3H, CH₃). EI-MS: 427 (M⁺), 419, 389, 354, 343, 83, 58.

Ethyl-2-amino-5-oxo-7,7-dimethyl-spiro[(4H)-5,6,7,8-tetrahydrochromene-4,3'-(3'H)-5'-chloro-indol]-(1'H)-2'-one-3-carboxylate (**4k**). IR (KBr, cm⁻¹): 3383, 3277, 3214, 2957,

1726, 1687, 1614, 1514, 1476, 1350, 1219, 1169, 1052, 907, 747. ¹H NMR (500 MHz, DMSO-d₆): δ 10.28 (s, 1H, NH), 7.90 (br. s, 2H, NH₂), 6.67–7.09 (m, 3H, ArH), 3.72 (q, $J = 7.3$ Hz, 2H, CH₂), 2.53 (m, 2H, CH₂), 2.14 (d, $J = 15.8$ Hz, 1H, CH_AH_B), 2.08 (d, $J = 15.7$ Hz, 1H, CH_AH_B), 1.00 (s, 3H, CH₃), 0.96 (s, 3H, CH₃), 0.81 (t, $J = 7.0$ Hz, 3H, CH₃). EI-MS: 416 (M⁺), 343, 153, 83, 55.

Ethyl-2-amino-5-oxo-7,7-dimethyl-spiro[(4H)-5,6,7,8-tetrahydrochromene-4,3'-(3'H)-5'-bromo-indol]-(1'H)-2'-one-3-carboxylate (**4l**). IR (KBr, cm⁻¹): 3386, 3276, 3213, 2955, 1726, 1686, 1612, 1512, 1474, 1350, 1216, 1165, 1050, 940, 746. ¹H NMR (500 MHz, DMSO-d₆): δ 10.29 (s, 1H, NH), 7.91 (br. s, 2H, NH₂), 6.64–7.22 (m, 3H, ArH), 3.72 (q, $J = 6.1$ Hz, 2H, CH₂), 2.53 (m, 2H, CH₂), 2.11 (d, $J = 15.7$ Hz, 1H, CH_AH_B), 2.09 (d, $J = 15.9$ Hz, 1H, CH_AH_B), 1.00 (s, 3H, CH₃), 0.96 (s, 3H, CH₃), 0.82 (t, $J = 7.1$ Hz, 3H, CH₃). EI-MS: 460 (M⁺), 444, 387 (100), 378.

Methyl-2-amino-5-oxo-7,7-dimethyl-spiro[(4H)-5,6,7,8-tetrahydrochromene-4,3'-(3'H)-1'-benzyl-indol]-(1'H)-2'-one-3-carboxylate (**4m**). IR (KBr, cm⁻¹): 3366, 2955, 1680, 1610, 1529, 1350, 1311, 1170, 1055, 744. ¹H NMR (500 MHz, DMSO-d₆): δ 7.90 (s, 1H, ArH), 7.59 (d, $J = 7.5$ Hz, 2H, ArH), 6.67–7.36 (m, 8H, ArH, NH₂), 4.88 (s, 2H, NCH₂), 3.05 (s, 3H, CH₃), 2.50–2.62 (m, 2H, CH₂), 2.07–2.19 (m, 2H, CH₂), 1.04 (s, 3H, CH₃), 0.99 (s, 3H, CH₃). EI-MS: 458 (M⁺), 399, 367, 291, 279, 91 (100).

2-Amino-5-oxo-7,7-dimethyl-spiro[(4H)-5,6,7,8-tetrahydrochromene-4,3'-(3'H)-1'-benzyl-5'-bromo-indol]-(1'H)-2'-one-3-carbonitrile (**4n**). IR (KBr, cm⁻¹): 3420, 3321, 3179, 3961, 2193, 1707, 1675, 1604, 1481, 1350, 1050, 813. ¹H NMR (500 MHz, DMSO-d₆): δ 7.47 (d, $J = 18$ Hz, 2H, ArH), 6.67–7.34 (m, 8H, ArH, NH₂), 4.92 (s, 2H, NCH₂), 2.58–2.62 (m, 2H, CH₂), 2.06–2.51 (m, 2H, CH₂), 1.05 (s, 6H, 2 CH₃). EI-MS: 503 (M⁺), 414, 365, 91 (100), 65, 55.

Ethyl-2-amino-5-oxo-7,7-dimethyl-spiro[(4H)-5,6,7,8-tetrahydrochromene-4,3'-(3'H)-1'-benzyl-5'-Bromo-indol]-(1'H)-2'-one-3-carboxylate (**4o**). IR (KBr, cm⁻¹): 3490, 3391, 3279, 2996, 2919, 1679, 1609, 1528, 1310, 1168, 814. ¹H NMR (500 MHz, DMSO-d₆): δ 8.01 (s, 1H, ArH), 7.56 (d, $J = 7.5$ Hz, 2H, ArH), 7.12–7.33 (m, 6H, ArH, NH₂), 6.64 (d, $J = 8$ Hz, 1H, ArH), 4.93 (d, $J = 16$ Hz, 1H, NCH₂), 4.72 (d,

$J = 15.5$ Hz, 1H, NCH₂), 3.79 (q, 2H, CH₂), 2.50–2.57 (m, 2H, CH₂), 2.13 (d, $J = 11$ Hz, 2H, CH₂), 1.02 (s, 3H, CH₃), 0.98 (s, 3H, CH₃), 0.55 (t, 3H, CH₃). EI-MS: 550 (M^+), 479, 461, 371, 91 (100), 65.

2-Amino-5-oxo-7,7-dimethyl-spiro[(4H)-5,6,7,8-tetrahydrochromene-4,3'-(3'H)-1'-allyl-indol]-(1'H)-2'-one-3-carbonitrile (**4p**). IR (KBr, cm⁻¹): 3374, 3311, 3147, 2961, 2879, 2192, 1722, 1658, 1606, 1470, 1349, 1220, 1054, 747. ¹H NMR (500 MHz, DMSO-d₆): δ 7.22 (s, 2H, NH₂), 7.12–7.15 (m, 1H, ArH), 6.97 (d, $J = 7$ Hz, 1H, ArH), 6.91–6.88 (m, 1H, ArH), 6.80 (d, $J = 7.5$ Hz, 1H, ArH), 5.52–5.61 (m, 1H, =CH), 4.85–4.94 (m, 2H, =CH₂), 4.34–4.44 (m, 2H, NCH₂), 2.50–2.57 (m, 2H, CH₂), 2.07–2.19 (m, 2H, CH₂), 1.04 (s, 3H, CH₃), 1.00 (s, 3H, CH₃). EI-MS: 375 (M^+), 335, 290, 251 (100), 223, 209, 194, 179, 140, 115, 55.

Ethyl-2-amino-5-oxo-7,7-dimethyl-spiro[(4H)-5,6,7,8-tetrahydrochromene-4,3'-(3'H)-1'-allyl-indol]-(1'H)-2'-one-3-carboxylate (**4q**). IR (KBr, cm⁻¹): 3351, 3261, 3191, 2962, 1688, 1615, 1528, 1350, 1309, 1222, 1052, 744. EI-MS: 422 (M^+), 381, 349 (100), 338, 309, 291, 83, 69, 55.

2 Results and Discussion

The XRD pattern of SBA-15 showed the (100), (110), and (200) reflections typical of an ordered mesoscopic structured silica [25] which exhibit a two-dimensional hexagonal symmetrical array of nano-channels (Fig. 1). NH₂-SBA-15 was also characterized by the same pattern, indicating that the grafting of APTES did not affect the structural integrity of SBA-15. The porosity and volumetric characteristics of the materials were evaluated by volumetric analyses. In both materials (Fig. 2), the “Type IV” N₂ adsorption-desorption isotherms with “H1-type” hysteresis corresponded to condensation and evaporation steps, and were characteristic of periodic mesoporous materials. The textural properties of SBA-15 and NH₂-SBA-15 have been summarized in Table 1. It is noteworthy that the surface

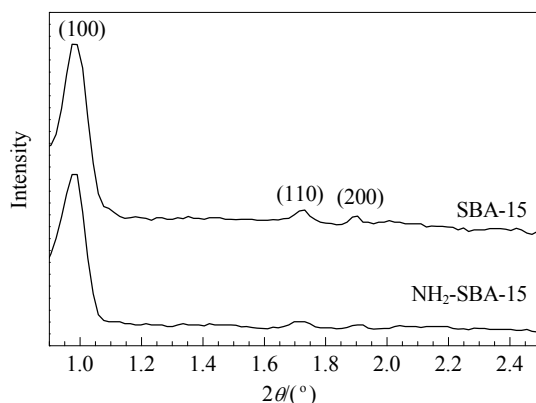


Fig. 1. Low-angle XRD patterns of SBA-15 and NH₂-SBA-15.

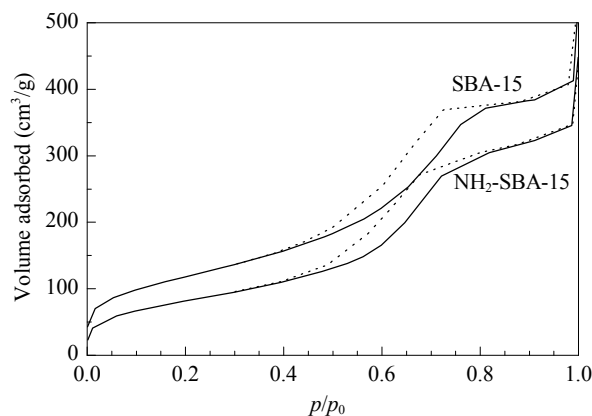


Fig. 2. Nitrogen adsorption-desorption isotherms of SBA-15 and NH₂-SBA-15.

area, pore volume, and pore size decreased following the modification, confirming that the surface modification occurred on the inner surface of the silica wall [23].

Table 1 Characteristics of the synthesized materials derived from nitrogen adsorption-desorption

Sample	$A_{BET}/(m^2/g)$	$V_{total}/(cm^3/g)$	D_{BJH}/nm
SBA-15	481	1.3	5.9
NH ₂ -SBA-15	356	1.0	3.6

The incorporation of organic groups into the SBA-15 framework was confirmed by the FT-IR spectra (Fig. 3). In both materials, bands around 811 and 1068 cm⁻¹ were seen which were subsequently assigned to the typical symmetric and asymmetric stretching of Si–O–Si caused by the condensed silica network [26]. The broad peak around 3392 cm⁻¹ was assigned to the O–H stretching vibration of the SiO–H and HO–H of adsorbed water. In the spectra of NH₂-SBA-15, the bands at 1405 and 1456 cm⁻¹ were assigning to the –(CH₂) bending vibration, whereas the peaks at 2908 and 2971 cm⁻¹ are attributed to C–H stretching vibrations in the methylene groups of the aliphatic chain [22],

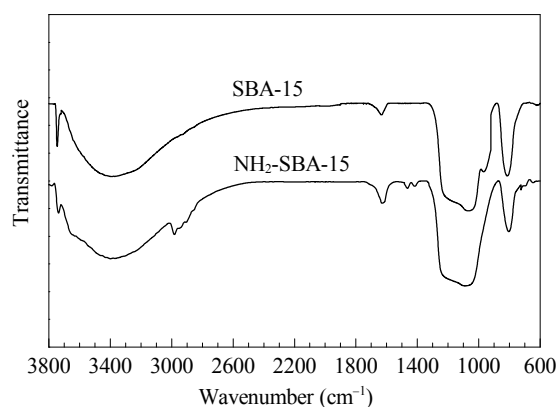


Fig. 3. FT-IR spectra of SBA-15 and NH₂-SBA-15.

indicating the presence of the anchoring APTES on the silica surface. Moreover, the absorption band at 1548 cm^{-1} , which almost overlapped with the bending vibration of the adsorbed H_2O , corresponded to the N–H bending vibration of the $-\text{NH}_2$ groups. Therefore, the FT-IR results confirmed the anchoring of the amine groups on the SBA-15 silica surface. The TEM image showed the parallel channels, which resembled the configuration of the pores in SBA-15 (Fig. 4). This indicated that the pores in NH_2 -SBA-15 had not collapsed during the functionalization reaction. This image was in good agreement with the XRD result for NH_2 -SBA-15.

As part of our ongoing interest in the application of heterogeneous solid catalysts in organic synthesis [27–29], herein we report a simple, efficient, and green method for the synthesis of spirooxindole derivatives with fused chromenes, through the three-component condensation of isatin, malononitrile, and dimedone using SBA-Pr- NH_2 as a nanocatalyst in an aqueous medium.

To establish our optimum conditions, we initially tried to prepare 2-amino-5-oxo-7,7-dimethyl-spiro[(4H)-5,6,7,8-tetrahydrochromene-4,3'-(3'H)-5'-bromo-indol]-(1'H)-2'-one-3-carbonitrile **4d** from the reaction of 5-bromo isatin **1** (2 mmol), malononitrile **2** (2 mmol), and dimedone **3** (2 mmol), which we identified as a model reaction, in the presence of SBA-Pr- NH_2 (0.02 g) under different conditions (Table 2). The most encouraging result was obtained when water was employed as the solvent in the presence of a catalytic amount of SBA-Pr- NH_2 under refluxing conditions. We decided to investigate the scope of the reaction further by employing a variety of differentially substituted isatins bearing different functionalities and cyanoacetic esters. The

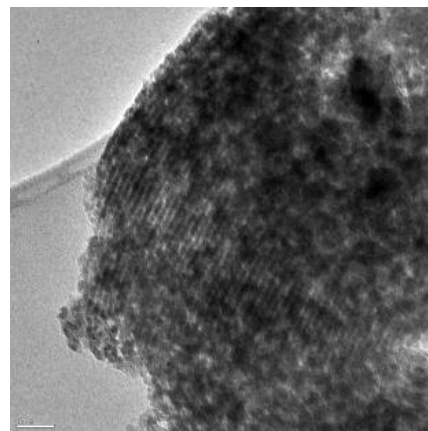


Fig. 4. TEM image of NH_2 -SBA-15.

Table 2 The optimization of the reaction conditions for the synthesis of compound **4d**

Entry	Solvent	Time (min)	Isolated yield (%)
1	H_2O	5	80
2	EtOH	60	84
3	EtOH/ H_2O (1:1)	90	73
4	CH_3CN	120	75
5	neat (140 °C)	180	96

corresponding spirooxindole compounds were obtained in high to excellent yields (78–94) after 5–50 min by simple filtration. The condensation reactions of cyanoacetic esters with isatin derivatives and dimedone were also found to give the desired products in high yields (Table 3). The progress of the reaction was monitored by TLC. Upon completion of the reaction, the mixture was cooled to room temperature and the crude product was filtered off and washed

Table 3 SBA-Pr- NH_2 catalyzed synthesis of spirooxindoles **4a–4q** in an aqueous medium

Entry	R^1	R^2	R^3	Product	Time (min)	Isolated yield (%)	Melting point (°C)	
							Found	Reported
1	H	H	CN	4a	5	91	258–260	268–270 [1]
2	NO_2	H	CN	4b	20	94	302–304	> 300 [30]
3	Cl	H	CN	4c	5	88	285–287	286–288 [30]
4	Br	H	CN	4d	5	80	302–304	305–307 [31]
5	H	H	CO_2Me	4e	5	79	237–239	230–232 [32]
6	NO_2	H	CO_2Me	4f	5	85	270–271	new
7	Cl	H	CO_2Me	4g	5	80	252–254	new
8	Br	H	CO_2Me	4h	5	79	262–264	new
9	H	H	CO_2Et	4i	10	78	260–261	257–258 [13]
10	NO_2	H	CO_2Et	4j	15	81	286–289	new
11	Cl	H	CO_2Et	4k	25	82	278–280	271–272 [30]
12	Br	H	CO_2Et	4l	10	83	247–248	260–262 [33]
13	H	benzyl	CO_2Me	4m	45	88	238–240	new
14	Br	benzyl	CN	4n	30	91	260–262	new
15	Br	benzyl	CO_2Et	4o	50	85	281–283	new
16	H	allyl	CN	4p	25	79	> 300	new
17	H	allyl	CO_2Et	4q	35	83	242–244	new

with H₂O. The resulting solid was then dissolved in hot ethanol and filtered to remove the catalyst. Subsequent cooling of the filtrate led the precipitation of pure crystals of the spirooxindole derivatives, which were collected by filtration. The recovered catalyst was then washed sequentially with a diluted aqueous Et₃N solution, water, and acetone, and dried under vacuum. The reusability of the catalyst was investigated under optimized conditions for the synthesis of the model compound **4a**. As shown in Fig. 5, the process of recycling was completed four times with no significant decrease in the activity of the catalyst. The yields for the four runs were found to be 91%, 86%, 81%, and 72%, respectively.

A possible mechanism for this reaction is shown in Scheme 3. SBA-Pr-NH₂ plays a crucial role in accelerating the reaction. The initiation step begins with the deprotonation of malononitrile or the cyanoacetic esters **2** by SBA-Pr-NH₂. It is reasonable to assume that compounds **4a–4q** result from the initial formation of the isatylidene malononitrile derivatives **7** according to the standard Knoevenagel reaction. Subsequent Michael-type addition of the enolic form of dimedone **6** to **7** gives the intermediate **8**

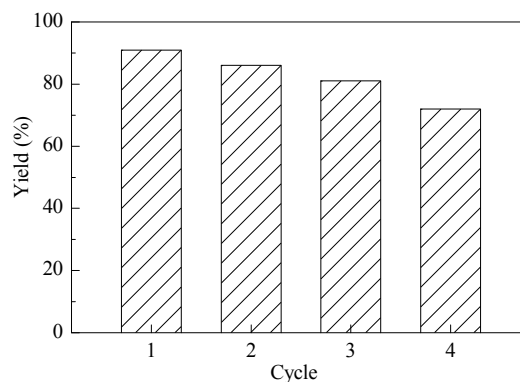
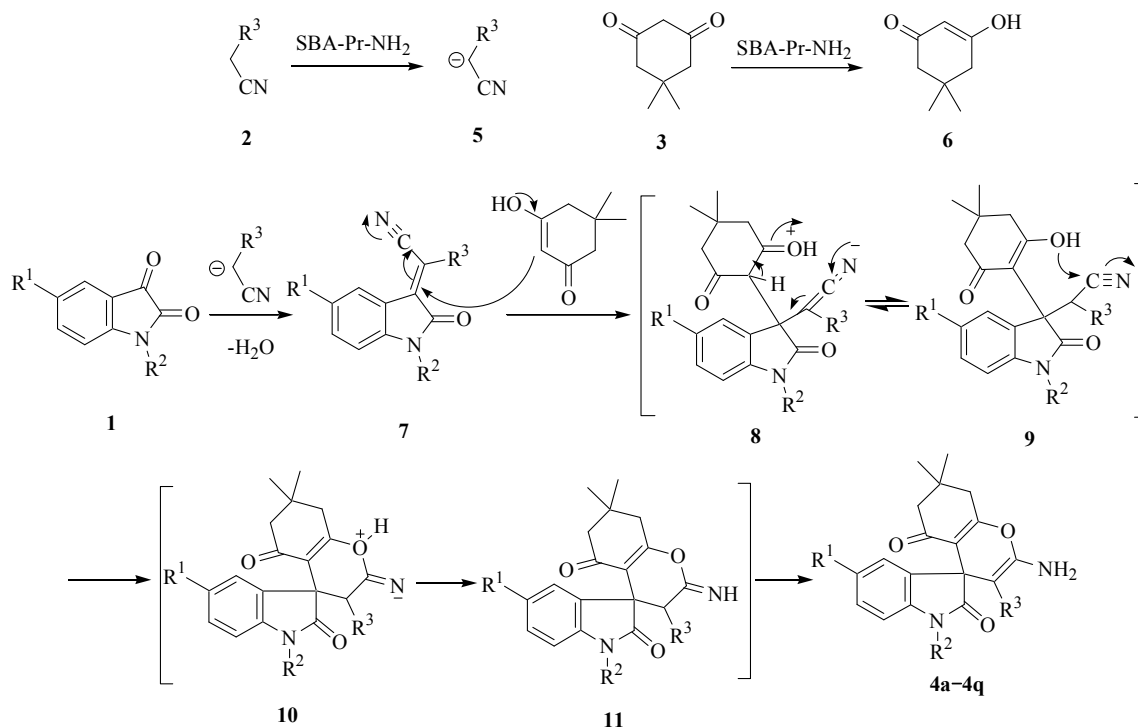


Fig. 5. Reusability of NH₂-SBA-15 in the synthesis of compound **4a**.

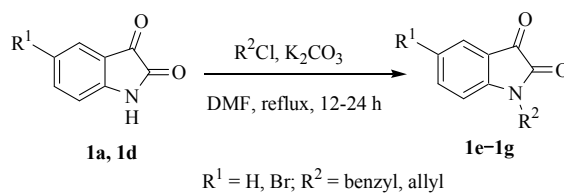
which affords the corresponding products **4a–4q** by cyclization of hydroxyl group to the cyano moiety (Scheme 3).

The synthesis of the *N*-alkyl isatins was performed by reacting the isatins with different alkyl halides in DMF in the presence of K₂CO₃ for 12–24 h (Scheme 4) [34]. The results are summarized in Table 4.

Several different conditions have been reported in the literature for the synthesis of spirooxindole derivatives, as



Scheme 3. Plausible mechanism for synthesis of spirooxindole derivatives **4a–4q** in the presence of SBA-Pr-NH₂.



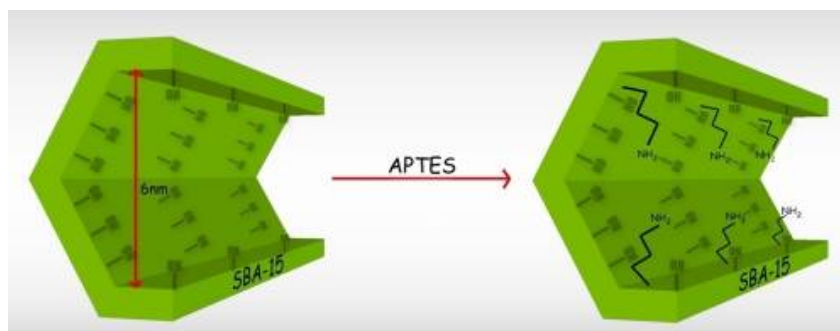
Scheme 4. Synthesis of *N*-alkylated isatins.

Table 4 Reaction times and yields of *N*-alkylated isatins **1e–1g**

Entry	R ¹	R ²	Product	Time (h)	Yield (%)	Melting point (°C)	
						Found	Reported
1	H	benzyl	1e	12	85	131–133	130–132 [35]
2	Br	benzyl	1f	24	70	147–150	152 [36]
3	H	allyl	1g	24	80	88–91	86–88 [37]

Table 5 Comparison of different conditions for the synthesis of spirooxindole **4a**

Entry	Catalyst	Solvent	Condition	Time (min)	Yield (%)	Year
1	—	EtOH	electrolysis	32	96	2007 [31]
2	InCl ₃	CH ₃ CN	reflux	90	75	2007 [10]
3	triethylbenzylammonium chloride	H ₂ O	heating	180	94	2007 [14]
4	tris(2-hydroxyethyl)amine	EtOH	heating	180	95	2008 [38]
5	tetra- <i>n</i> -butylammonium fluoride	H ₂ O	reflux	30	97	2008 [11]
6	NEt ₃	EtOH	reflux	30	83	2008 [39]
7	β-Cyclodextrin	H ₂ O	heating	300	90	2009 [12]
8	Ethylenediamine diacetate	H ₂ O	heating	60	90	2010 [15]
9	sodium stearate	H ₂ O	heating	180	95	2010 [40]
10	lipase	EtOH	heating	180	94	2011 [30]
11	tetra- <i>n</i> -butylammonium bromide	—	heating	40	90	2011 [41]
12	SBA-Pr-NH ₂	H ₂ O	reflux	5	91	this work

**Fig. 7.** APTES grafting on the SBA-15 surface.

shown in Table 5. In contrast to the existing methods, the current methodology offers several advantages, such as a simpler procedure, shorter reaction times, facile synthesis, simpler work-up, higher yields, and greener conditions.

The preparation of SBA-15 as a new nanoporous silica can be achieved using the commercially available triblock copolymer Pluronic P123 as a structure directing agent [42]. The amino functionalized SBA-15 was typically synthesized through post-grafting. A schematic illustration of the preparation of SBA-Pr-NH₂ is shown in Fig. 7. The calcined SBA-15 silica was functionalized with APTES to provide SBA-Pr-NH₂ as solid basic nanocatalyst.

3 Conclusions

We have described an efficient one-pot three-component reaction of isatins with malononitrile or cyanoacetic esters and dimedone for the synthesis of spirooxindole derivatives,

catalyzed by SBA-Pr-NH₂ in an aqueous medium. The current method does not involve any hazardous organic solvents and the mild reaction conditions and simplicity of the procedure provide significant improvements over many of the other existing methods. We have established SBA-Pr-NH₂ as an efficient heterogeneous solid basic catalyst that can be easily handled and removed from the reaction mixture by simple filtration. Short reaction times and high product yields under our reaction conditions clearly demonstrate the advantages of using SBA-Pr-NH₂ as a nanocatalyst for this reaction.

Acknowledgements

We gratefully acknowledge for financial support from the Research Councils at Alzahra University and the University of Tehran.

References

- 1 Longeon A, Guyot M, Vacelet J. *Experientia*, 1990, **46**: 548
- 2 Trost B M, Brennan M K. *Synthesis*, 2009: 3003
- 3 Kang TH, Matsumoto K, Tohda M, Murakami Y, Takayama H, Kitajima M, Aimi N, Watanabe H. *Eur J Pharmacol*, 2002, **444**: 39
- 4 Cui C-B, Kakeya H, Osada H. *Tetrahedron*, 1996, **52**: 12651
- 5 Bhaskar G, Arun Y, Balachandran C, Saikumar C, Perumal P T. *Eur J Med Chem*, 2012, **51**: 79
- 6 Jiang X, Sun Y, Yao J, Cao Y, Kai M, He N, Zhang X, Wang Y, Wang R. *Adv Synth Catal*, 2012, **354**: 917
- 7 Galliford C V, Scheidt K A. *Angew Chem, Int Ed*, 2007, **46**: 8748
- 8 Da Silva J F M, Garden S J, Pinto A C. *J Braz Chem Soc*, 2001, **12**: 273
- 9 Lashgari N, Mohammadi Ziarani G. *Arkivoc*, 2012, **i**: 277
- 10 Shanthi G, Subbulakshmi G, Perumal P T. *Tetrahedron*, 2007, **63**: 2057
- 11 Gao S, Tsai C H, Tseng C, Yao C F. *Tetrahedron*, 2008, **64**: 9143
- 12 Sridhar R, Srinivas B, Madhav B, Reddy V P, Nageswar Y V D, Rao K R. *Can J Chem*, 2009, **87**: 1704
- 13 Dabiri M, Bahramnejad M, Baghbanzadeh M. *Tetrahedron*, 2009, **65**: 9443
- 14 Zhu S-L, Ji S-J, Zhang Y. *Tetrahedron*, 2007, **63**: 9365
- 15 Hari G S, Lee Y R. *Synthesis*, 2010: 453
- 16 Tang T, Zhao Y, Xu Y, Wu D, Xu J, Deng F. *Appl Surf Sci*, 2011, **257**: 6004
- 17 Yasmin T, Müller K. *J Chromatogr A*, 2011, **1218**: 6464
- 18 Song S W, Hidajat K, Kawi S. *Langmuir*, 2005, **21**: 9568
- 19 Ziarani G M, Badiei A R, Khaniania Y, Haddadpour M. *Iran J Chem Chem Eng*, 2010, **29**(2): 1
- 20 Chen S Y, Huang C Y, Yokoi T, Tang C Y, Huang S J, Lee J J, Chan J C C, Tatsumi T, Cheng S. *J Mater Chem*, 2012, **22**: 2233
- 21 Sujandi, Prasetyanto E A, Park S E. *Appl Catal A*, 2008, **350**: 244
- 22 Shahbazi A, Younesi H, Badiei A. *Chem Eng J*, 2011, **168**: 505
- 23 Badiei A, Goldoos H, Ziarani G M. *Appl Surf Sci*, 2011, **257**: 4912
- 24 Chong M A S, Zhao X S. *J Phys Chem B*, 2003, **107**: 12650
- 25 Zhao D, Huo Q, Feng J, Chmelka B F, Stucky G D. *J Am Chem Soc*, 1998, **120**: 6024
- 26 Badiei A, Goldoos H, Ziarani G M, Abbasi A. *J Colloid Interface Sci*, 2011, **357**: 63
- 27 Mohammadi Ziarani G, Badiei A, Hassanzadeh M, Mousavi S. *Arabian J Chem*, 2012, in press
- 28 Mohammadi Ziarani G, Badiei A, Haddadpour M. *Int J Chem*, 2011, **3**(1): 87
- 29 Mohammadi Ziarani G, Badiei A, Shahjafari F, Pourjafar T. *S Afr J Chem*, 2012, **65**: 10
- 30 Chai S-J, Lai Y-F, Xu J-C, Zheng H, Zhu Q, Zhang P-F. *Adv Synth Catal*, 2011, **353**: 371
- 31 Elinson M N, Ilovaisky A I, Dorofeev A S, Merkulova V M, Stepanov N O, Miloserdov F M, Ogibin Y N, Nikishin G I. *Tetrahedron*, 2007, **63**: 10543
- 32 Li Y, Chen H, Shi C, Shi D, Ji S. *J Comb Chem*, 2010, **12**: 231
- 33 Singh Raghuvanshi D, Nand Singh K. *J Heterocycl Chem*, 2010, **47**: 1323
- 34 Schmidt M S, Reverdito A M, Kremenchuzky L, Perillo I A, Blanco M M. *Molecules*, 2008, **13**: 831
- 35 Marti C, Carreira E M. *J Am Chem Soc*, 2005, **127**: 11505
- 36 Majumdar K C, Kundu A K, Chatterjee P. *J Chem Res Synop*, 1996: 460
- 37 Ukrainets I V, Bereznyakova N L, Gorokhova O V, Shishkina S V. *Chem Heterocycl Compd*, 2009, **45**: 1241
- 38 Shemchuk L A, Chernykh V P, Red'kin R G. *Russ J Org Chem*, 2008, **44**: 1789
- 39 Mortikov V Y, Litvinov Y M, Shestopalov A A, Rodinovskaya L A, Shestopalov A M. *Russ Chem Bull Int Ed*, 2008, **57**: 2373
- 40 Wang L-M, Jiao N, Qiu J, Yu J-J, Liu J-Q, Guo F-L, Liu Y. *Tetrahedron*, 2010, **66**: 339
- 41 Mobinikhaledi A, Foroughifar N, Bodaghi Fard M A. *Synth Commun*, 2011, **41**: 441
- 42 Zhao D, Feng J, Huo Q, Melosh N, Fredrickson G H, Chmelka B F, Stucky G D. *Science*, 1998, **279**: 548